Studies of membranotropic and fusogenic activity of two putative HCV fusion peptides

Simon Gonzalez, Florian Gallier, Sabrina Kellouche, Franck Carreiras, Ettore Novellino, Alfonso Carotenuto, Gérard Chassaing, Paolo Rovero, Jacques Uziel, Nadege Lubin-Germain

Studies of membranotropic and fusogenic activity of two putative HCV fusion peptides

Simon Gonzalez,[a] Florian Gallier,[a] Sabrina Kellouche,[b] Franck Carreiras,[b] Ettore Novellino,[c] Alfonso Carotenuto,[c] Gérard Chassaing,[d] Paolo Rovero,[e] Jacques Uziel,[a] Nadège Lubin-Germain[a]

a Laboratoire de Chimie Biologique, University of Cergy-Pontoise, 5 mail Gay-Lussac, Cergy-Pontoise, France,

b Equipe de Recherche sur les Relations Matrice Extracellulaire-Cellules, ERRMECe (EA1391), Institut des Matériaux, I-MAT (FD4122), University of Cergy-Pontoise, MIR, rue Descartes, 95031 Neuville sur Oise Cedex, France.

c Department of Pharmacy, University of Naples 'Federico II', Naples 80131, Italy

d Sorbonne Universités, UPMC University Paris 06, LBM, 4 place Jussieu, F-75005, Paris, France

e French-Italian Interdepartmental Laboratory of Peptide and Protein Chemistry and Biology, University of Florence, 50019, Sesto Fiorentino, Italy

ARTICLE INFO

Keywords:

HCV Fusion peptides

Spectrofluorescence

Membranotropic properties

Fusogenic properties

Microscopy

Abstract

Over the past decades, membranotropic peptides such as positively charged cell-penetrating peptides (CPPs) or amphipathic antimicrobial peptides (AMPs) have received increasing interest in order to improve therapeutic agents cellular uptake.

As far as we are concerned, we were interested in studying HCV fusion peptides as putative anchors. Two peptides, HCV6 and HCV7, were identified and conjugated to a fluorescent tag NBD and tested for their interaction with liposomes as model membranes. DSC and spectrofluorescence analyses demonstrate HCV7 propensity to insert or internalize in vesicles containing anionic lipids DMPG whereas no activity was observed with zwitterionic DMPC. This behavior could be explained by the peptide sequence containing a cationic arginine residue. On the contrary, HCV6 did not exhibit any

membranotropic activity but was the only sequence able to induce liposomes' fusion or aggregation monitored by spectrofluorescence and DLS. This two peptides mild activity was related to their inefficient structuration in contact with membrane mimetics, which was demonstrated by CD and NMR experiments.

Altogether, our data allowed us to identify two promising membrane-active peptides from E1 and E2 HCV viral proteins, one fusogenic (HCV6) and the other membranotropic (HCV7). The latter was also confirmed by fluorescence microscopy with CHO cells, indicating that HCV7 could cross the plasma membrane *via* an endocytosis process. Therefore, this study provides new evidences supporting the identification of HCV6 as the HCV fusion peptide as well as insights on a novel membranotropic peptide from the HCV-E2 viral protein.

1. Introduction

1.1. Fusion peptide and cell-penetration

Since the discovery of the first cell-penetrating peptides (CPPs), Tat and penetratin in the 90s, membranotropic peptides have been of increasing interest for enhancing therapeutic agent cellular uptake.[1–4] Even if their mechanism of action is still controversial, the different sequences identified over the years, being CPPs or AMPs, shared particular properties. Indeed, these membranotropic sequences are generally amphipathic, composed of hydrophobic and cationic residues. Thus, they are usually classified as primary amphipathic peptides, where the amphipathicity is due to primary structure, and secondary amphipathic peptides, where a particular folding gives two distinct cationic and hydrophobic faces.

Another class of membrane-active peptides is fusion peptides. They differ from CPPs or AMPs as they are generally hydrophobic, thus allowing membrane insertion during the fusion process. This membrane activity could be interesting for enhancing cell penetration as described for gene delivery.[5]

Hence, we propose to study different putative HCV fusion peptides as possible cell-penetrating agents, based on their propensity to interact with lipidic membranes (highlighted by DSC analyses), their conformations in membrane mimetic environments (CD and NMR) their membranotropic activity on liposomes as cell membrane models (studied by spectrofluorescence) and on epithelial cells (microscopy), and finally their ability to induce liposomes fusion (spectrofluorescence by FRET and DLS).

1.2. HCV fusion proteins

HCV is an enveloped RNA virus of the *Flaviviridae* family. The virus counts 10 different viral proteins: 4 structural proteins (Core, p7, E1 and E2) and 6 non-structural proteins (NS2, NS3, NS4A, NS4B, NS5A and NS5B).[6] While non-structural proteins have different roles during viral replication (protease, polymerase), structural proteins and particularly E1 and E2 are responsible for the first crucial steps of the infection being cells' receptors interaction (generally entailed by E2) as well as fusion. The two proteins E1 and E2 are thus called fusion proteins (FPs).[7] Several studies suggest that E1 and E2 could act as truncated class II FPs[8] which involves an E1/E2 heterodimer and a pH-dependent mechanism, including fusion peptide exposure and insertion in cell membrane.[9,10]

1.3. Selected sequences

A large number of studies have been carried out in order to identify the HCV fusion peptide, using mutagenesis and membrane behavior studies such as fusion or hemifusion experiments. For instance, Drummer *et al.*[11] have demonstrated that the ^{284}VFLV^{288}G sequence in E1 could be important for fusion since mutations in this region did not change protein production, dimer formation or receptor recognition but strongly impaired the viral fusion activity.

Pérez-Berná *et al.*[12] also investigated the fusogenic activity of different 11-mer peptides corresponding to E1 and E2 overlapping sequences. Each peptide was tested in fusion and hemifusion assays which allowed the authors to clearly identify several membranotropic regions, particularly E1 (276-286) and E2 (418-432). In another study using spectrofluorescence and ^{31}P-NMR,[13] the same authors confirmed that E1 (274-291) is capable to interact and to modify lipidic membranes of different compositions through electrostatic and hydrophobic interactions. We opted for this consensual E1 (276-286) peptide. Moreover, more regions in the ectodomain of the hepatitis C virus envelope glycoprotein E2 (430–449, 543–560 and 603–624) were identified.[14] But we have retained the (418-432) sequence in first intention.[15]

Based on the literature, two HCV fusion peptides (Table 1) namely **HCV1** and **HCV2** (Entries 1 and 2) are putative fusion sequences. Both contain Cys residues which could disturb the membrane interaction study by side-product formation due to disulfide-bridge creation. Since these Cys residues are unlikely involved in intra or inter disulfide bridge within the protein,[16] they were replaced by Ser residues in **HCV1** and **HCV2** giving these peptides named **HCV3** and **HCV7** (Entries 3 and 5). Finally, the **HCV3** sequence was truncated in order to improve solubility and facilitate conjugation with a cargo, giving the sequence **HCV6** (Entry 4). The **Tat** peptide (Entry 6), derived from the HIV Tat protein, was chosen as a reference since its membranotropic activity and its propensity to cross the plasma membrane have been studied in the literature.[17,18]

Entry	Name	Code	Sequences
1	HCV-E1(265-304)	**HCV1**	LVGSATLCSALYVGDLCGSVFLVGQLFTFSPRRHWTTQDC
2	HCV-E2(418-432)	**HCV2**	SWHINRTALNCNDS
3	[^{272}Ser, ^{281}Ser, ^{304}Ser] HCV-E1(265-304)	**HCV3**	LVGSATL<u>S</u>SALYVGDL<u>S</u>GSVFLVGQLFTFSPRRHWTTQD<u>S</u>
4	[^{281}Ser]HCV-E1(276-286)	**HCV6**	YVGDL<u>S</u>GSVFL
5	[^{429}Ser]HCV-E2(418-432)	**HCV7**	SWHINRTALN<u>S</u>NDS
6	HIV-Tat(47-57)	**Tat**	YGRKKRRQRRR

Table 1: Selected HCV fusion sequences and Tat as a reference. Underlined residues correspond to Ser in place of Cys in native sequences.

The free peptides were also decorated with two different patterns (Table 2): a hydrophilic linker TTDS in order to increase solubility and a fluorescent tag NBD in order to perform spectrofluorescence assays and fluorescence microscopy. In the case of **HCV6-NT** and **HCV7-N** (Entries 3 and 4), the peptide was labeled on a Lys side-chain in order to keep the free amino-group for enhancing water solubility.

Entry	Peptide	Patterns	Structure	Code
1	Tat	NBD	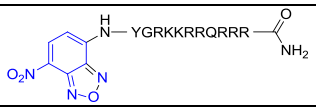	**Tat-N**
2	Tat	NBD-TTDS-	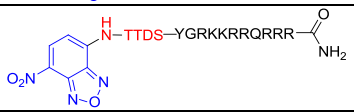	**Tat-NT**
3	HCV6	NBD-TTDS-	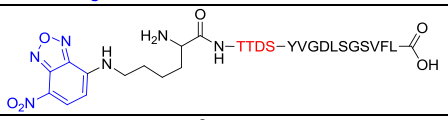	**HCV6-NT**
4	HCV7	NBD	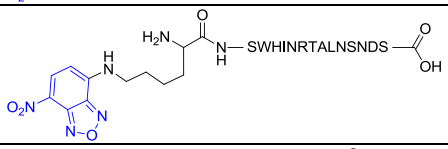	**HCV7-N**
5	HCV7	NBD-TTDS-	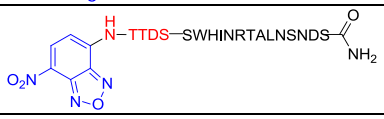	**HCV7-NT**

Table 2: Modified Tat and HCV peptide sequences

2. Experimental

2.1. Materials

HPLC-MS analyses were performed on an Alliance Chromatography (Waters) apparatus with a Phenomenex Kinetex C18 column (2.6µm, 3.0 × 100 mm) using a 0.6 mL/min flowrate, with the indicated linear gradients (see supporting information), coupled to a single quadrupole ESI-MS (Micromass ZQ). The solvent systems used were: A (0.1% TFA in H_2O) and B (0.1 % TFA in ACN). UPLC-MS analyses were performed on a Waters Acquity UPLC apparatus, which was equipped with a Waters Acquity UPLC BEH C18 column (1.7 µm, 2.1 × 50 mm) using a 0.6 mL/min flowrate, with the indicated linear gradients (see supporting information), coupled to a single quadrupole ESI-MS (Waters 3100 Mass Detector). The solvent systems used were: A (0.1% TFA in H_2O) and B (0.1 % TFA in ACN).

2.2. Peptide synthesis

All peptides were synthesized either on a 0.1, 0.05 or 0.025-mmol scale by a high-efficiency solid-phase peptide synthesis (SPPS) strategy, using a Liberty Blue automated microwave synthesizer (CEM Corporation, Matthews, NC, USA) following the Fmoc/*t*Bu methodology. The reactions were performed in a Teflon vessel and mixed by N_2 bubbling. Reaction temperatures were monitored by an internal fiber optic sensor. Usual amino-acid side chain's protecting groups were used and coupling steps were performed with DIC and Oxyma Pure in DMF.

After peptide elongation, pegylation was performed manually in a plastic syringe and continuously stirred by orbital shaking. The coupling step was performed using Fmoc-TTDS-OH (2.5 eq), TBTU (2.5 eq) and DIPEA (3.5 eq) for 30 min at room temperature. The reaction completion was confirmed by Kaiser Test and/or micro-cleavage.

Conjugation with the fluorophore was performed manually in a plastic syringe and continuously stirred by orbital shaking. The coupling step was performed using NBD (4 eq) and DIPEA (10 eq) for

18 h at room temperature and protected from light using an aluminum foil. The reaction completion was confirmed by micro-cleavage.

In the case of **HCV6-NT** or **HCV7-N**, NBD was introduced on a Lys side-chain using a modified procedure. After peptide elongation, Fmoc-Lys(Dde)-OH (5 eq) was manually coupled on the *N-ter* position using TBTU (5 eq) and DIPEA (7 eq) for 30 min at room temperature. The Dde protecting group was selectively removed using a 3M/2.25M NH_2OH.HCl/imidazole solution in NMP/DMF 5/1 (v/v) added to the resin and stirred at room temperature for 3h. After washing with DMF, the NBD was coupled on Lys side-chain as described above.

All peptides were then cleaved by a TFA/H_2O/TIS (95/2.5/2.5) solution at room temperature for 2 to 4h. After precipitation in cold diethyl ether and freeze-drying, peptides were purified by semi-preparative RP-HPLC and analyzed by UPLC-MS.

2.3. Circular dichroism

All CD spectra were recorded using a JASCO J715 spectropolarimeter at 25 °C with a cell of 1 mm path length. The CD spectra were acquired by the range from 260 nm to 190 nm, 1 nm bandwidth, 4 accumulations, and 100 nm/min scanning speed. The CD spectra of **HCV6** and **HCV7**, at a concentration of 30 µM, were acquired in water (pH=7.4), and in DPC (20 mM) micellar solutions. HCV7 CD spectrum was also acquired in SDS solution (20 mM). Secondary structure content was predicted from CD spectra using the Jasco Secondary Structure Estimation tool (Jasco Inc.), the Contin-LL method[19] and the BeStSel method[20,21] (Table 3).

2.4. NMR

NMR Spectroscopy. 99.9% ^2H_2O were obtained from Aldrich (Milwaukee, USA), 98% DPC-d_{38} was obtained from Cambridge Isotope Laboratories, Inc. (Andover, USA), [(2,2,3,3-tetradeuterio-3-(trimethylsilanyl)]propionic acid (TSP) from MSD Isotopes (Montreal, Canada). The samples for NMR spectroscopy were prepared by dissolving the appropriate amount of peptide in 0.54 ml of ^1H_2O (pH 5.5), 0.06 ml of ^2H_2O to obtain a concentration 2 mM and 200 mM of DPC-d_{38}. NMR spectra were recorded on a Varian INOVA 700 MHz spectrometer equipped with a z-gradient 5 mm triple-resonance probe head. All the spectra were recorded at a temperature of 25 °C. The spectra were calibrated relative to TSP (0.00 ppm) as internal standard. One-dimensional (1D) NMR spectra were recorded in the Fourier mode with quadrature detection. The water signal was suppressed by gradient echo.[22] Two dimensional (2D) DQF-COSY,[23,24] TOCSY,[25] and NOESY[26] spectra were recorded in the phase-sensitive mode using the method from States.[27] Data block sizes were 2048 addresses in t_2 and 512 equidistant t_1 values. Before Fourier transformation, the time domain data matrices were multiplied by shifted $\sin^2$ functions in both dimensions. A mixing time of 70 ms was used for the TOCSY experiments. NOESY experiments were run with mixing time of 100 ms. The qualitative and quantitative analyses of DQF-COSY, TOCSY, and NOESY spectra, were obtained using the interactive program package XEASY.[28] Complete ^1H NMR chemical shift assignments were effectively achieved for **HCV7** according to the Wüthrich procedure[29] via the usual systematic application of DQF-COSY, TOCSY, and NOESY experiments with the support of the XEASY software package (Supporting Information, Table S1). $^3J_{\alpha N}$ coupling constants were measured by 1D proton and DQF-COSY spectra. The temperature coefficients of the amide proton chemical shifts were calculated from 1D ^1H NMR and 2D TOCSY experiments performed at different temperatures in the range 25-40°C by means of linear regression. Observed NOEs are reported in Figure S1 (Supporting Information).

2.5. Liposomes preparation

Depending on the desired composition, a lipid solution in chloroform (DOPG, DOPC, DMPC, POPC, POPE, POPS), in ethanol (sphingomyelin), in methanol (cholesterol) or in chloroform/methanol/water 65/38/8 (v/v/v) (DMPG) was introduced in a round-bottom flask. Organic solvents were removed slowly under vacuum at 30°C with the aid of a rotary evaporator, and the residue was then placed under high vacuum for at least 4 h. The lipids were hydrated with a buffer solution (10 mM Tris, 100 mM NaCl, pH 7.3 or 10 mM PBS, 100 mM NaCl, pH 7.4) for at least 30 min above the transition temperature (T_m) to obtain a multilamellar vesicles (MLVs) suspension of the desired concentration. The turbid suspension was subsequently extruded eight times through a 200 nm polycarbonate track-etch membrane (Whatman) and ten times through a 100 nm polycarbonate track-etch membrane (Whatman) with a 10 mL Thermobarrel extruder (Lipex Biomembranes). The resulting 100-nm-diameter large unilamellar vesicles (LUVs) suspension was stored at 4°C and used within one week. Vesicular size and distribution were evaluated by light scattering (Zetasizer Nano, Malvern) considering the following parameters: n = 1.345 ; Absorption = 0.001 ; water as solvent.

Total phosphate concentration was titrated thanks to the Bartlett method.[30]

2.6. Differential Scanning Calorimetry

DSC experiments were performed on a MicroSC calorimeter (Setaram Instrumentation). For each analysis, three scans from 40°C to 5°C were performed with a scan rate of 1°C/min and waiting 15 min between sequential scans in a series to allow thermal equilibration. Data analysis was performed by the Calisto Software provided by Setaram Instrumentation and with Origin software. The MLVs suspensions were prepared as described above reaching a concentration of 5 mM in Tris Buffer (10 mM Tris, 100 mM NaCl, pH 7.3). Aliquots of peptide solution (concentration varying from 300 µM to 1 mM) in Tris buffer (with 5% DMSO for experiments with **HCV6**) were gradually added to the lipid MLVs to obtain peptide/lipid molar ratios of 1/100, 1/50, 1/25, and finally 1/10. For each addition, the exact same volume of Tris buffer solution was used as a reference.

2.7. Membranotropic and fusogenic studies

2.7.1. Internalization in LUVs

Time-course fluorescence measurements were recorded with a Jasco Fluorescence Spectrophotometer at the desired temperature (controlled by a Jasco MCB-100 mini circulation bath). As an excitation source, a Xenon lamp was used at 460 nm and emission was measured at 555 nm. The excitation bandwidth was set to 10 nm and the emission to 2.5 nm. Depending on the sequence, the PMT voltage was set between 650 and 750 V. To avoid peptide adsorption and subsequent fluorescence quenching, polymethacrylate cuvettes were used. During measurement, the solution was stirred at 800 rpm.

For each analysis, 3 mL of PBS buffer (10 mM phosphate, 100 mM NaCl, pH 7.4) and 30 µL of a 1 mM LUVs solution was introduced in a spectrophotometer cuvette. The emission measured at 555 nm was used as a blank value. 3 µL of a 100 µM solution of peptide bearing the NBD fluorescent tag (75 µL of a 4 µM solution for **HCV6-NT** and 18.5 µL of a 16 µM solution for **HCV7-NT**) was added into the cuvette and incubated at the desired temperature for 10-15 min. The solution was then cooled to 10°C and 30 µL of a concentrated (~1M) sodium dithionite (DT) solution was added for reduction.

Experiments with a diluted DT solution were performed following the same procedure but after cooling to 10°C, several aliquots of increasing volume (3, 3, 6, 12, 24, 48, 48 and 100 µL) of a 100

mM DT solution were added for reduction. Finally, several aliquots of 100 mM DT were added, until the blank value was reached.

2.7.2. Fusion assays by FRET

Fusion/hemifusion experiments using FRET were performed on a Jasco fluorescence spectrophotometer at 37°C for experiments with LM3 (POPC/POPE/POPS/sphingomyelin/cholesterol 10/5/2/2/10) LUVs (controlled by a Jasco MCB-100 mini circulation bath). A Xenon lamp was used at 450 nm and emission was measured at 530 nm for time-course fluorescence measurements. The excitation bandwidth was set to 10 nm and the emission to 2.5 nm and the PMT voltage was set at 600V. Analyses were performed using polymethacrylate cuvettes. During measurement, the solution was stirred at 800 rpm.

For each experiment, 1.7 mL of 10 mM phosphate buffer without NaCl (pH 7.4), 27 µL of a 1mM LM3 LUVs solution containing 2% mol Rho-DPPE and 2% mol NBD-DPPE, and 273 µL of a 1 mM LM3 LUVs solution (yielding a 1/10 ratio between fluorescent LUVs and non-fluorescent ones) were added into a spectrophotometer cuvette. The fluorescence emission measured at 530 nm was used as a blank value. 60 µL of a 100 µM peptide solution (77 µL of a 78 µM solution for **HCV6** and 24 µL of a 1 mM solution for acetyl-penetratin Ac-Pen) was added yielding a peptide/lipid ratio of 1/50 (1/12 for Ac-Pen). The fluorescence emission at 530 nm was then recorded for 10 to 20 min. Cuvettes were then placed in a 37°C bath under stirring and fluorescence emission at 530 nm was measured after one night. A LUVs solution without peptide was studied following the same procedure as a control experiment.

2.8. Dynamic light scattering

Fusion/hemifusion experiments by DLS were performed using a Zeta-Sizer Nano (Malvern) considering the following parameters: n = 1.345 ; Absorption = 0.001 ; water as solvent. The samples were analyzed at 37°C.

For each sample, 1.7 mL of 10 mM phosphate buffer without NaCl (pH 7.4), and 300 µL of a 1mM LM3 LUVs solution (POPC/POPE/POPS/sphingomyelin/cholesterol 10/5/2/2/10) were poured into a screw-cap tube yielding a final concentration of 150 µM. 60 µL of a 100 µM peptide solution (77 µL of a 78 µM solution for **HCV6** and 24 µL of a 1 mM solution for Ac-Pen) was added yielding a peptide/lipid ratio 1/50 (1/12 for Ac-Pen). The samples were placed in a 37°C bath under stirring (800 rpm), and polydispersity and vesicle size (in intensity) were measured after 20 min and one night.

After one night, the same volume of peptide solution was added to the samples, and polydispersity and size were again measured after another 20 min and one night.

A LUVs solution without peptide was studied following the same procedure as a control experiment.

2.9. Microscopy

Chinese Hamster Ovarian cells (CHO, ATCC) were grown in HAM F12 medium (Invitrogen) supplemented with 10% fetal calf serum in a humidified atmosphere with 5% CO_2 at 37 °C. For experiments, cells were harvested with 0.5% trypsin-EDTA (Invitrogen), then seeded onto glass coverslips at a density of 25 000 cells/cm^2 and incubated in culture medium for 24 h until sub-confluence.

Cells were incubated with 400 µL of a (100 µM for **Tat-NT** and 25 µM for **HCV7-N**) peptide TFA-free solution (removed by several freeze-dryings with HCl 100 mM) in PBS buffer (10 mM phosphate, 100 mM NaCl, pH 7.4) for 30 min or 1 h at 37°C. Cells were fixed with 3% paraformaldehyde for 10 minutes and washed with PBS. After washing, cell nuclei were stained with DAPI (4,6-diamidino-2-phenylindole dihydrochloride, D9542, Sigma Aldrich) at 0.3µg/ml. Coverslips were mounted in Prolong® Gold Antifade Reagent (P36930, Invitrogen). Staining was examined with fluorescence conventional microscopy (Leica MLB). All pictures were acquired using a x63 zoom and analyzed with Image J software.

3. Results

3.1. Structural analyses

3.1.1. Circular dichroism

To explore the conformational behavior of **HCV6** and **HCV7**, we performed a CD study of these peptides in water, and DPC/water solutions. The last medium is commonly used as rough mimetic of zwitterionic membrane environment.[31] CD spectrum of **HCV6** in water (Figure 1a) reveals the prevalence of β-structures (β-turns and β-strands from about 35 to 50%) together with random conformations. Upon the addition of 20 mM of DPC micelles, the CD spectrum clearly changed indicating that the interactions of **HCV6** with the micelle do occur. A single wide minimum at 208 nm could be observed in this environment.

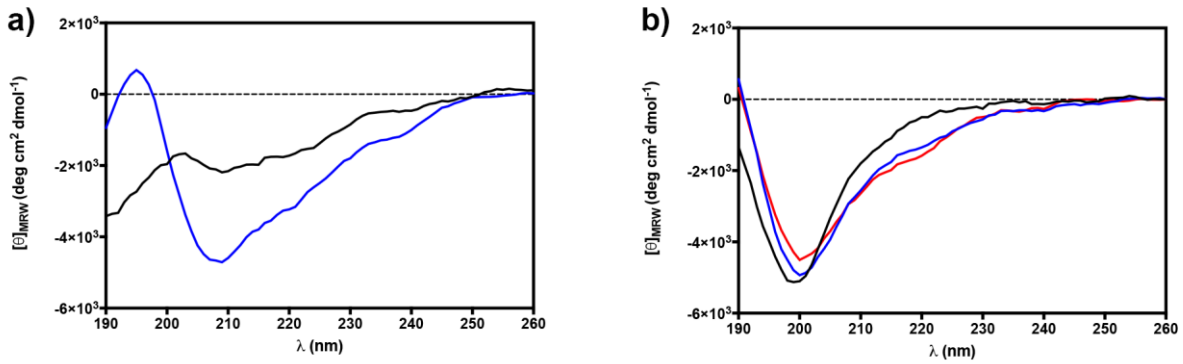

Figure 1: CD spectra of HCV6 (a) and HCV7 (b) in water (black line), DPC (blue line), and SDS (red line). HCV peptides concentration 30 µM in water (pH=7.4) and in DPC (20 mM) micellar solutions. HCV7 CD spectrum was also acquired in SDS solution (20 mM)

Secondary structure evaluation (Table 3) gave different results. ContinLL and BeStSel estimated an increase of the helical content, while Jasco tool estimated an increase of the β-strand structure. Unfortunately, we could not discern between the two conformations by NMR investigation (see below) due to the low solubility of **HCV6**.

Peptide (medium)	**α-helix**	**β-strand**	**β-turn**	**Random coil**
HCV6 (water)	9.3[a]/11.1[b]/14.7[c]	31.2[a]/17.0[b]/18.4[c]	22.2[a]/18.5[b]/15.6[c]	37.3[a]/53.3[b]/51.3[c]
HCV6 (DPC)	12.9 [a]/32.5[b]/33.5[c]	42.3[a]/4.2[b]/17.4[c]	13.0[a]/18.3[b]/6.6[c]	31.9[a]/45.0[b]/42.5[c]

HCV7 (water)	0.0[a]/4.7[b]/0.0[c]	27.8[a]/30.9[b]/42.5[c]	15.9[a]/17.8[b]/13.8[c]	56.3[a]/46.6[b]/43.7[c]
HCV7 (DPC)	0.0[a]/5.2[b]/0.0[c]	43.5[a]/30.2[b]/42.3[c]	5.5[a]/18.1[b]/14.5[c]	50.9[a]/46.5[b]/43.2[c]
HCV7 (SDS)	0.0[a]/4.6[b]/42.8[c]	50.1[a]/31.6[b]/14.1[c]	4.1[a]/18.7[b]/43.1[c]	45.8[a]/45.1[b]/43.1[c]

Table 3: Percentage of secondary structure from CD spectra
Secondary structure content was predicted from CD spectra using [a] the Jasco Secondary Structure Estimation tool (Jasco Inc.), [b]the Contin-LL method and [c] the BeStSel method

CD spectrum in water of **HCV7** revealed the presence of disordered conformers with a minimum close to 198 nm (Figure 1b). In DPC micelles solution, the spectra of **HCV7** showed a reduction and a shift towards higher wavelength of the minimum (from 198 to 201 nm) with the appearance of a wide shoulder around 220 nm. This increase of ordered structure content as confirmed by the secondary structure estimations reported in Table 3. **HCV7** was also investigated in SDS micelles as mimetic of negatively charged membranes,[32,33] since DSC results highlighted its propensity to interact with negative membranes. CD spectrum acquired in SDS is very similar to that obtained in DPC with minimal differences pointing to a further stabilization of the turn/strand structures.

3.1.2. NMR

Conformational preferences of **HCV7** in DPC micelles were also investigated by solution NMR. Unfortunately, low water solubility (< 50 µM) of **HCV6** prevented the NMR analysis of this peptide. NMR parameters of **HCV7** (Table S1) indicated a high degree of flexibility of this peptide in solution. In particular, the observed $^{3}J_{\alpha N}$ couplings range between 6.3 and 7.7 Hz except for Alanine residue and the Wishart-Sykes chemical shift indexes[34] based on the observed Hα chemical shifts predict no regular α-helix or β-sheet structures. A few NOEs between Hα and HN protons of residues i and i+2 (Figure S1) indicate the presence of β-turn structures mainly in the central and C-terminal part of the peptide (residues 6-13) as confirmed by the relatively low HN temperature coefficients of residues 9, 10, and 13. However, the exiguous number of the overall NOE correlations (Figure S1), again indicating structural flexibility, prevented the calculation of an NMR-based 3D structure of the peptide.

3.2. Differential scanning calorimetry

In order to characterize the effect of **HCV6** and **HCV7** on lipidic membranes, DSC analyses with zwitterionic (PC) and anionic (PG) MLVs were performed. Indeed, PC is one of the most representative membrane lipids in the biological membrane (more than 50%)[35] and therefore constitute an appropriate model. The cell membrane is also composed of anionic lipids such as PI or PS, but at lower levels. PG is rarely found in eukaryotic membranes but has been considered as a good representative for PI, PS or other anionic membrane components (such as GAGs) in order to study electrostatic interactions. The biological membrane shows a high diversity in the lipid's chains composition with a majority of unsaturated fatty acids. However, since the phase transition of a membrane composed of unsaturated lipids is below 0°C, such lipids are irrelevant for DSC analyses. Hence, we chose to work with C_{14} lipids such as dimyristoyl phosphatidylcholine (DMPC) and dimyristoyl phosphatidylglycerol (DMPG) since their phase transition occurs near room temperature thus facilitating the experiments.

Thermograms illustrating the effect of **Tat**, **HCV6,** and **HCV7** on DMPG are represented in Figure 2 and thermodynamic parameters for MLVs with 1/100 and 1/25 P/L ratios are presented in Table 4. The **Tat** peptide was studied as a reference considering its well-known membranotropic activity, particularly on membranes composed of anionic lipids due to a bidentate interaction between guanidinium groups of arginine residues and phosphate.[36]

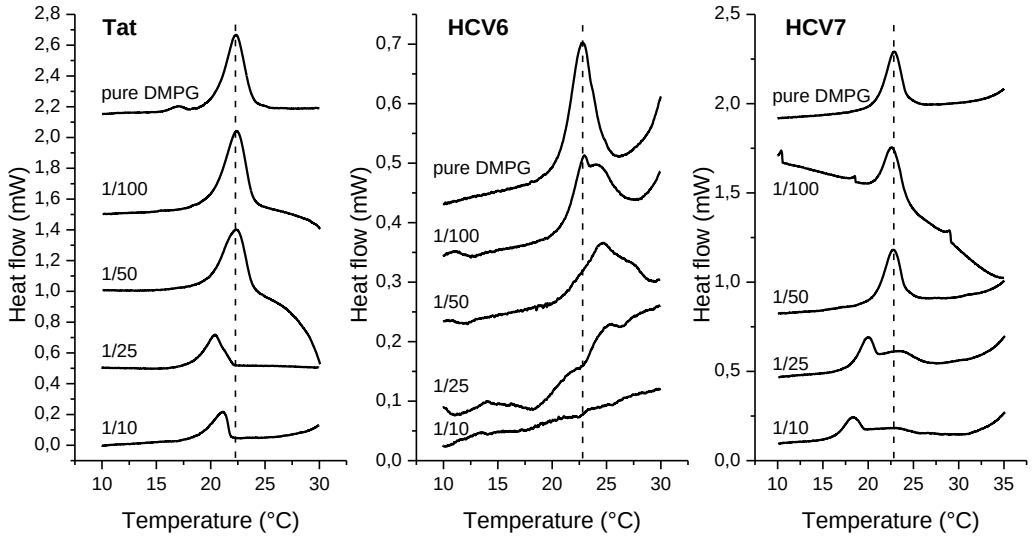

Figure 2: Thermograms illustrating the effect of Tat**,** HCV6, **and** HCV7 **on MLVs 5 mM membranes composed of DMPG. Aliquots of peptide solution (concentration varying from 300 µM to 1 mM) in Tris buffer (with 5% DMSO for experiments with HCV6) were gradually added to the lipid MLVs to obtain peptide/lipid molar ratios of 1/100, 1/50, 1/25, and finally 1/10.**

The obtained results for **Tat** are in accordance with the literature since the thermograms show an endothermic event around 23°C corresponding to the transition from the P_{β}' ripple phase to the L_{α} fluid phase (also called the main transition). The first peptide additions, yielding to P/L ratios of 1/100 and 1/50, did not affect the main transition which was still measured around 23°C. The other two additions, yielding to a P/L ratio of 1/25 and 1/10 respectively, lead to an important decrease in T_m indicating that Tat interacts more efficiently with the fluid phase than the gel phase and that the peptide is able to promote fluid domains within the lipidic membrane. The enthalpy modification induced by **Tat** demonstrates its propensity to insert in the membrane hydrophobic core and to disturb lipids acyl chain packing.

Peptide	P/L ratio	ΔH (kcal/mol)	T_m (°C)
Tat	1/100	-7.26 ± 0.06	22.38 ± 0.02
	1/25	-3.02 ± 0.01	20.32 ± 0.11
HCV6	1/100	-4.16 ± 0.40	22.95 ± 0.02 ; 24.07 ± 0.79
	1/25	-1.04 ± 0.23	25.04 ± 0.25
HCV7	1/100	-5.31 ± 0.35	22.91 ± 0.06
	1/25	-4.80 ± 0.10	19.92 ± 0.16 ; 22.93 ± 0.20

Table 4: Thermodynamic results obtained by DSC with MLVs of DMPG.
MLV concentration 5 mM in Tris Buffer. Experiments with HCV6 were performed using 5% peptide DMSO solution. Data analysis was performed by the Calisto Software provided by Setaram Instrumentation and with Origin software

The same experiment performed with **HCV6** (Table 4) gives unexpected results. Indeed, because of its supposed overall negative charge, **HCV6** should not be able to interact with a membrane composed of anionic lipids due to electrostatic repulsion, but the thermograms obtained show an increase in T_m at a P/L ratio of 1/50. This increase implies a modification of the thermotropic membrane behavior and that the peptide is able to enhance gel domain formation in the lipidic layer. Nevertheless, one should note that the experiments were performed using 5% DMSO peptide solution because of the low solubility of **HCV6** in water. An experiment performed with a DMSO-free solution at a P/L ratio of 1/50 did not exhibit any modification in T_m (data not shown) indicating that the observed thermotropic behavior could be largely imputed to the presence of an organic solvent or its combined effect with **HCV6**. For this reason, modification in enthalpy induced by **HCV6** will not be discussed here.

On the contrary, **HCV7** (Table 4 and Figure 2) seems to be more active as a membranotropic peptide. Indeed, the thermograms obtained with MLVs composed of DMPG show a significant decrease in T_m at a P/L ratio of 1/25 and 1/10 (to 19.92°C and 18.17°C respectively). As described for Tat, these observations highlight the propensity of **HCV7** to interact with a membrane composed of DMPG (probably due to electrostatic interactions resulting from the arginine residue) and its ability to promote fluidic behavior. Interestingly, thermograms also display a second endothermic transition, with a more important width, corresponding to the initial main transition temperature. This observation could indicate that **HCV7** is able to interact with DMPG in a cooperative manner, yielding fluidic peptide-rich domains and unmodified peptide-poor domains. The overall enthalpy (corresponding to both phase transitions combined) is only slightly modified (0.51 kJ/mol) which implies that if **HCV7** is able to interact with lipid head groups and to modify membrane fluidity, it may not be able to efficiently insert in the membrane and to disturb the lipid acyl chains packing.

Because of **HCV6** poor solubility in water and **HCV7** promising activity, further experiments were only performed with **HCV7**, considered as our "lead". Thus, its interaction with a membrane composed of zwitterionic lipids such as DMPC was also investigated by DSC analyses (Figure 3).

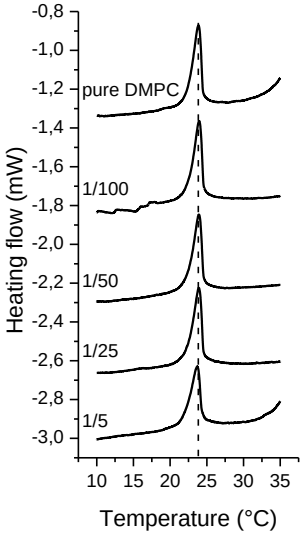

Figure 3: Thermogram illustrating the effect of HCV7 on MLVs membrane composed of DMPC. The initial main transition is represented by a dashed line. Aliquots of peptide solution (concentration varying from 300 µM to 1 mM) in Tris buffer were gradually added to the lipid MLVs to obtain peptide/lipid molar ratios of 1/100, 1/50, 1/25, and finally 1/5.

The resulting thermograms did not show any significant effect on the membrane behavior (either in terms of T_m or ΔH as shown in Table 5), even after a peptide addition yielding to a P/L ratio of 1/5. Considering the previous results, it appears that electrostatic interactions are crucial for **HCV7** membranotropic activity, probably because of the arginine residue. In order to characterize the peptide behavior in more biologically relevant conditions, DSC analyses were also performed with a membrane containing less anionic lipids: MLVs composed of a mixture DMPC/DMPG 9/1. The thermograms (data not shown) did not display any modification in T_m or ΔH implying that **HCV7** needs more than 10 % anionic residues in the membrane in order to efficiently disturb its properties.

Peptide	P/L ratio	ΔH (kcal/mol)	T_m (°C)
HCV7	1/100	-5.79 ± 0.04	23.93 ± 0.01
	1/25	-5.78 ± 0.24	23.89 ± 0.03

Table 5: Thermodynamic results obtained by DSC with MLVs of DMPC and HCV7. Data analysis was performed by the Calisto Software provided by Setaram Instrumentation and with Origin software

Overall, the results indicate that **HCV7** is able to interact with the lipidic membrane, more effectively with anionic lipids than zwitterionic ones. The data also show that this sequence could act in a cooperative way in contact with the membrane, which creates fluidic domains.

3.3. Spectrofluorescence

3.3.1. Internalization in liposomes

In order to characterize the membrane behavior of **HCV6** and **HCV7**, internalization assays with LUVs were performed and monitored by spectrofluorescence. This technique, described by Swiecicki *et al.*,[37] involves peptides conjugated to a fluorescent tag NBD, which is chemically reduced during the experiment. The reduction performed with sodium dithionite (DT) at 10°C transforms the NBD

nitro group into an amino group, which leads to complete loss of fluorescence. Monitoring the fluorescence intensity by time-course measurement displays a decrease which could be directly related to the percentage of peptide in solution. Since the reductive agent is unlikely able to cross the membrane at low temperature, the remaining fluorescence corresponds to peptides either internalized or inserted in LUVs membrane (Figure 4).

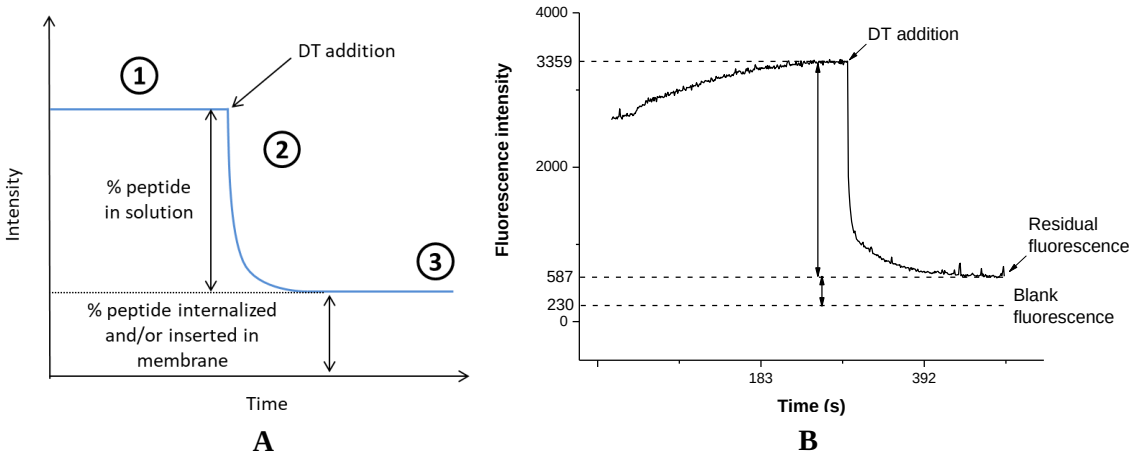

Figure 4: (A) Monitoring NBD fluorescence intensity (555 nm) during internalization assays. (1) Intensity at 10°C; (2) addition of reductive agent DT and decrease in fluorescence intensity; (3) Residual fluorescence corresponding to peptide internalized and/or inserted in LUVs membrane. (B) Experimental time-course measurement for Tat-NT **and DMPC/DMPG 9/1 LUVs.**

In order to prevent possible perturbations of the peptide/membrane interaction and to increase the solubility in water, the fluorescent tag NBD was initially coupled on a hydrophilic linker (TTDS), introduced at peptide *N*-terminus. The first result obtained with LUVs composed of DMPC/DMPG 9/1 and the **Tat** peptide as a reference (Table 6) confirms the ability of such cationic sequence to interact with anionic membrane and to penetrate the intravesicular medium.

Peptide	Incubation temperature	% peptide internalized and/or inserted
Tat-NT	37°C	18 ± 3
	24°C	25 ± 4
HCV6-NT	37°C	0
	24°C	0
HCV7-NT	37°C	0
	24°C	0

Table 6: Results of internalization experiments with pegylated peptides Tat, HCV6-NT, **and** HCV7-NT**, and LUVs of DMPC/DMPG 9/1 at 555nm. 3 µL of a 100 µM solution of peptide bearing the NBD fluorescent tag (75 µL of a 4 µM solution for HCV6-NT and 18.5 µL of a 16 µM solution for HCV7-NT) was added into the cuvette containing LUV (10 mM phosphate, 100 mM NaCl, pH 7.4 and 30 µL of a 1 mM LUVs solution) and incubated at the desired temperature for 10-15 min. The solution was then cooled to 10°C and 30 µL of a concentrated (~1M) sodium dithionite (DT) solution was added for reduction.**

Interestingly, the ability of **Tat** to cross the lipidic bilayer seems higher at T_m (24°C) than in fluid phase (37°C). Since the membrane is composed of several fluid and gel domains at T_m, separated by so-called phase-defects, this observation could be related to the importance of such permeabilized domains for peptide insertion and/or internalization as it has already been described.[38,39] **HCV6-NT** and **HCV7-NT** did not exhibit any membranotropic activity since all fluorescence was quenched after DT addition indicating that the peptide is only present in solution. However, this result could also be explained by the presence of the hydrophilic TTDS linker. Indeed, due to its length, the NBD fluorophore may no longer be protected from the reduction, even though the peptide is inserted in the membrane. The fluorescence would then be quenched just as if it was in solution.

To investigate the influence of TTDS linker, we have also tested the **Tat** peptide with NBD directly introduced at the peptide *N*-terminus (**Tat-N**, Entry 1 Table 2). The result obtained with LUVs of DMPC/DMPG 9/1 at 24°C (Table 7) show a better peptide internalization which could be consistent with our hypothesis. Since TTDS is a very hydrophilic linker, it could also interfere with the peptide internalization. For these reasons, **HCV7-N** (Entry 4 Table 2) was redesigned without the TTDS linker. The first results obtained with the new designed fluorescent **HCV7-N** and LUVs of different compositions demonstrate its propensity to interact with the lipidic membrane (Table 7).

Peptide	LUVs composition	% peptide internalized and/or inserted in the membrane
Tat-N	DMPC/DMPG 9/1	55 ± 6
HCV7-N	DMPC	0
	DMPG	8
	DMPC/DMPG 9/1	33

Table 7: Results obtained during internalization assays using tagged peptides incubated at 24°C, 555nm. 3 µL of a 100 µM solution of peptide bearing the NBD fluorescent tag (75 µL of a 4 µM solution for HCV6-NT and 18.5 µL of a 16 µM solution for HCV7-NT) was added into the cuvette containing LUV (10 mM phosphate, 100 mM NaCl, pH 7.4 and 30 µL of a 1 mM LUVs solution) and cooled to 10°C for 10-15 min.before adding 30 µL of a concentrated (~1M) sodium dithionite (DT) solution.

Hence, the fusion peptide **HCV7-N** membranotropic activity seems influenced by the proportion of anionic lipid DMPG since no activity could be observed with pure DMPC while membrane insertion and/or internalization are observed with different content of DMPG. This conclusion is consistent with the DSC analyses, showing a significant membrane modification induced by **HCV7** on vesicles composed of DMPG.

However, the reproducibility of these results remains problematic and can be explained by several hypotheses (Figure 5) : *(i)* the peptide could be adsorbed on the vesicle surface through electrostatic interaction, rather than inserted in the lipidic membrane, explaining why the NBD becomes accessible to reduction by large quantities of DT which are then able to diffuse more easily through the electrical double layer (Case A); *(ii)* the peptide could exist in several conformations in contact with the membrane, as it has already been demonstrated by structural analyses, and some conformations could be more sensitive to reduction than others (Case B); *(iii)* the peptide could be involved in a partition equilibrium between the membrane and solution indicating that, depending on the time, a different amount of inserted/internalized peptide could be measured after reduction (Case C). We are unable to

distinguish one of the hypotheses and certainly a critical concentration of DT close to the membrane, the accessibility of the NBD (conformations, equilibrium) are additional factors.

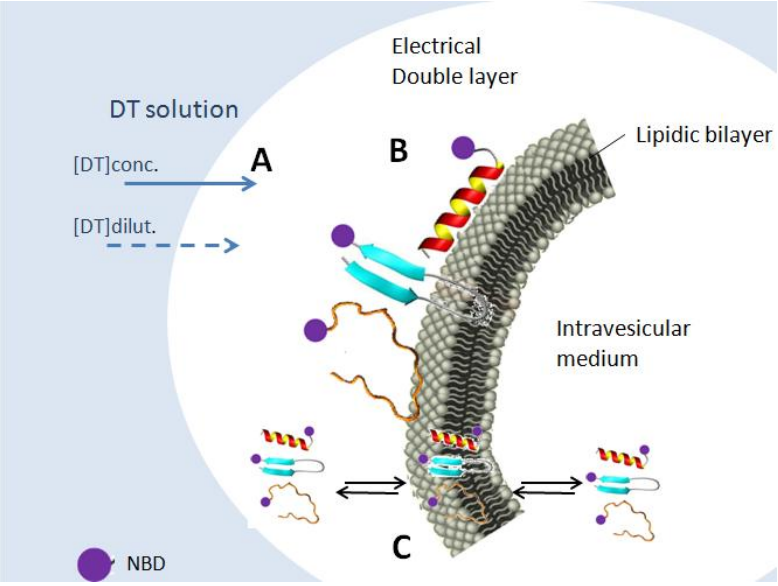

Figure 5: Different hypotheses explaining the lack of reproducibility in fluorescence assays: (A) Influence of DT concentration on diffusion through the electrical double bilayer; (B) Different peptide structures in contact with the membrane; (C) Partition equilibrium between the solution and the membrane

In order to investigate the influence of DT concentration, we performed a new experiment with several additions of diluted DT solution (Figure 6) performed at 10°C. The obtained result on **HCV7-N** showed no fluorescence intensity decrease during the first additions until the effective concentration (244 µL of diluted DT solution in total) is reached. A significant decline after the threshold is observed up to a value corresponding to 8% of the initial intensity that could correspond to 8% of peptide insertion/internalization. This could imply that a certain DT concentration is needed to observe the proper NBD reduction. Further DT addition results in complete loss of fluorescence which confirms our hypotheses as an important excess of reductive agent could explain discrepancies in results observed with this sequence. Therefore, this experiment seems consistent with the influence of DT concentration on the diffusion to achieve a complete reduction (Figure 5 case A).

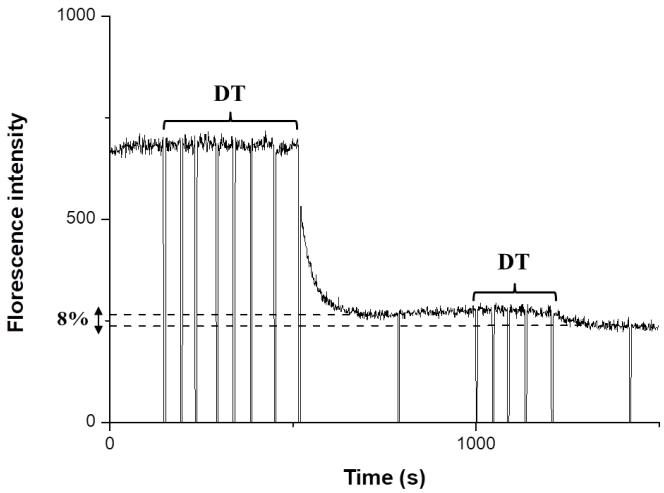

Figure 6: Experiment HCV7/LUVs DMPC/DMPG 7/3 with diluted DT solution. First additions were performed with increasing volumes of a 100 mM DT solution (3, 3, 6, 12, 24, 48, 48, 100 µL) at 10°C. Finally, several aliquots of the same solution were added, until the blank value was reached.

3.3.2. Fusion by FRET

In order to characterize the fusogenic activity of modified HCV fusion peptides, we also performed spectrofluorescence assays involving FRET. In this technique, first described by Struck *et al.* and applied in several studies,[40,41] LUVs are labeled by two fluorescent tags (one donor, NBD, and one acceptor, the rhodamine B (Rho)) allowing the FRET between them. After peptide addition, if fusion or aggregation is observed, the FRET efficiency decrease and an increase in NBD fluorescence intensity is observed. The peptide fusion activity could then be observed by following the fluorescence intensity at 530 nm.

In order to use biologically relevant lipid composition[42] and to compare our results with the literature, we performed our analysis with LM3 LUVs (POPC/POPE/POPS/SM/Chol 10/5/2/2/10) and in the conditions described by Wadhwani *et al.*[41] This composition reflects the cholesterol and lipid headgroup composition of the plasma membranes of H9 cells.

As already described, the addition of **Tat** peptide leads to spontaneous LUVs aggregation or even precipitation, indicating that this sequence is not a suitable reference to follow the fusion phenomenon. For this reason, we also used a sequence described as fusogenic by Wadhani *et al.*, the acetylated penetratin (**Ac-Pen**).[41,43] The different P/L ratios tested resulted in no or low fluorescence intensity increase until reaching the 1/12 value (Figure 7). The intensity measured after 1h30 was 842, much higher than the value corresponding to LUVs alone (330), thus demonstrating the fusion/aggregation induced by **Ac-Pen**. Interestingly, the observed phenomenon occurred at low rates. Indeed, the fluorescence intensity continues to rise after peptide addition until reaching a stable value (1280) after 4h.

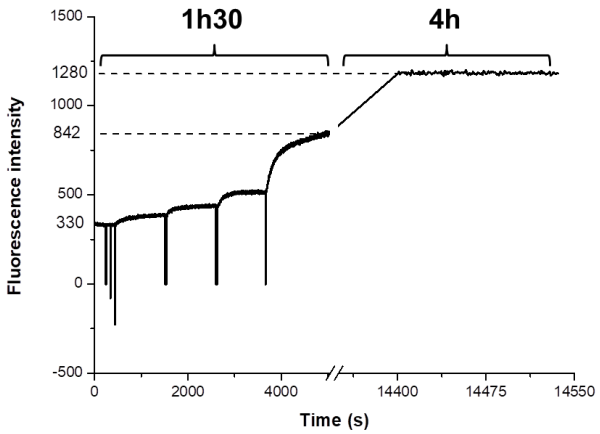

Figure 7: Fusion induced by Ac-Pen monitored by FRET To a solution of 1.7 mL of 10 mM phosphate buffer without NaCl (pH 7.4), 27 µL of a 1mM LM3 LUVs solution containing 2% mol Rho-DPPE and 2% mol NBD-DPPE, and 273 µL of a 1 mM LM3 LUVs solution (yielding a 1/10 ratio between fluorescent LUVs and non-fluorescent ones) were added. 60 µL of a 100 µM peptide solution (24 µL of a 1 mM solution for acetyl-penetratin Ac-Pen (peptide/lipid ratio of 1/12). The fluorescence emission at 530 nm was then recorded for 10 to 20 min at 37°C under stirring and fluorescence emission at 530 nm was measured after one night.

The different HCV fusion sequences, **HCV6** and **HCV7**, were then tested in the same conditions and no fluorescence increase was observed 10 min after peptide addition. As the phenomenon observed

with **Ac-Pen** seems to be relatively slow, the fluorescence was also measured after one night (Figure 8). For the two HCV sequences, the value (565 for **HCV7**) was higher than LUVs alone but lower than the intensity reached with **Ac-Pen**. This observation demonstrates that **HCV7** and **HCV6** could act as a fusogenic sequence involving a very slow phenomenon.

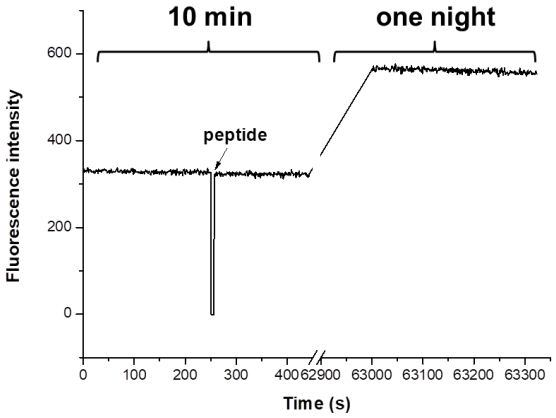

Figure 8: Fusion induced by HCV7 monitored by FRET. To a solution of 1.7 mL of 10 mM phosphate buffer without NaCl (pH 7.4), 27 µL of a 1mM LM3 LUVs solution containing 2% mol Rho-DPPE and 2% mol NBD-DPPE, and 273 µL of a 1 mM LM3 LUVs solution (yielding a 1/10 ratio between fluorescent LUVs and non-fluorescent ones) were added. 60 µL of a 100 µM peptide solution (77 µL of a 78 µM solution for HCV7 **(peptide/lipid ratio of 1/50). The fluorescence emission at 530 nm was then recorded for 10 to 20 min at 37°C under stirring and fluorescence emission at 530 nm was measured after one night.**

In order to check if the fluorescence increase observed after one night at 37°C was not due to experimental conditions or artifacts, a control experiment involving LUVs alone was carried out in the same conditions. The results obtained show no fluorescence intensity increase after 10 min but a significantly higher value after one night. This observation could imply a slow fusion and/or aggregation phenomenon in these conditions, even without peptide. Interestingly, **HCV6** and **HCV7** lead to slightly higher intensity values than the control experiment after one night (*After 10 min, ** after 1 night

Table 8). Even if the difference may not be significant, this observation could imply that these two sequences have a low fusogenic activity in these conditions. This phenomenon should thus be confirmed by another technique such as dynamic light scattering.

Sequence	Intensity *	Intensity**
Ac-Pen	842	1340
HCV6	323	581
HCV7	326	565
/	324	480

*After 10 min, ** after 1 night

Table 8: Fluorescence intensity at 530 nm for each experiment performed at 37°C for experiments with LM3 (POPC/POPE/POPS/sphingomyelin/cholesterol 10/5/2/2/10) LUVs (controlled by a Jasco MCB-100 mini circulation bath). A Xenon lamp was used at 450 nm and emission was measured at 530 nm for time-course fluorescence measurements. The excitation bandwidth was set to 10 nm and the emission to 2.5 nm and the PMT voltage was set at 600V.

3.4. Dynamic light scattering

The fusogenic activity was also characterized by DLS using LM3 LUVs and free peptides in the same conditions than FRET assays. After a first peptide addition reaching a P/L ratio of 1/50, vesicle size is measured by DLS after 20 min and one night. Another addition is then performed (reaching a 1/12 ratio) and two more measurements are performed (corresponding to 24 h and two days since the first addition).

As expected, **Ac-Pen** induces a significant size increase 20 min after the first peptide addition (reaching 180.4 ± 11.5 nm instead of 136.5 ± 10.3 nm for LUVs alone), demonstrating a possible fast fusion/aggregation phenomenon (Figure 9A). Interestingly, the control experiment performed with LUVs alone did not display any vesicle size increase, indicating that the liposomes are unlikely able to fuse or aggregate in these conditions (Figure 9B) conversely to what was observed during FRET assays.

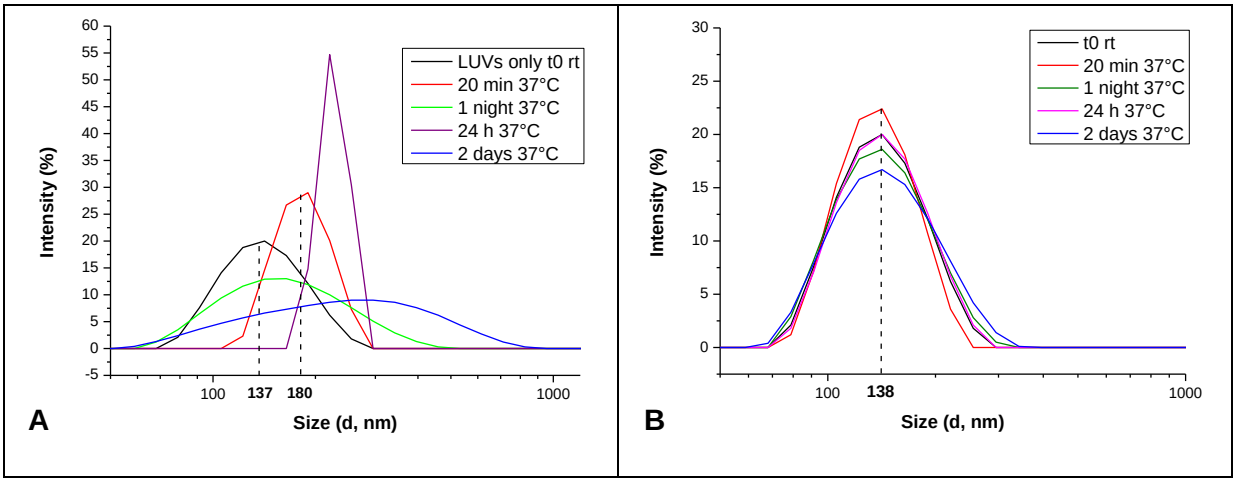

Figure 9: DLS analysis of LM3 LUVs in presence of Ac-Pen **(A); and alone as a control experiment (B). At 1.7 mL of 10 mM phosphate buffer without NaCl (pH 7.4), and 300 µL of a 1mM LM3 LUVs solution (POPC/POPE/POPS/sphingomyelin/cholesterol 10/5/2/2/10) with a final concentration of 150 µM was added 24 µL of a 1 mM solution for Ac-Pen yielding a peptide/lipid ratio 1/12. At 37°C under stirring (800 rpm), polydispersity and vesicle size (in intensity) were measured after 20 min and one night.**

Among the HCV sequences, only **HCV6** shows a significant vesicle size increase from 141.6 ± 8.1 nm for LUVs alone to 220.3 ± 14.7 nm (Figure 10). This observation demonstrates that the **HCV6** peptide is able to induce vesicle fusion or aggregation and is consistent with the behavior described with FRET spectrofluorescence. Indeed, the only significant size increase is noticed after the second peptide addition and 2 days after the first one, indicating a low and slow fusogenic or aggregation activity.

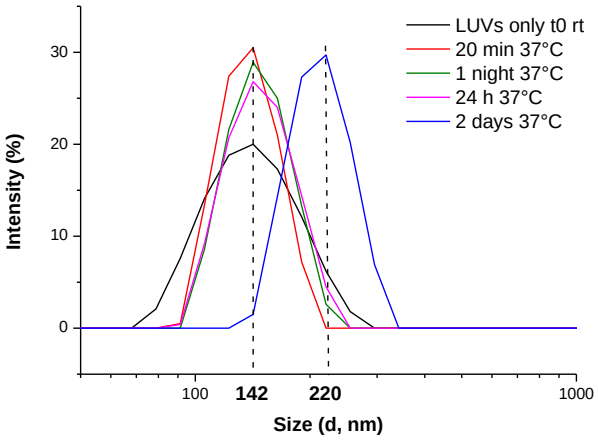

Figure 10: DLS analysis of LM3 LUVs in presence of HCV6. **At 1.7 mL of 10 mM phosphate buffer without NaCl (pH 7.4), and 300 µL of a 1mM LM3 LUVs solution (POPC/POPE/POPS/sphingomyelin/cholesterol 10/5/2/2/10) with a final concentration of 150 µM was added 77 µL of a 78 µM solution of** HCV6 **yielding a peptide/lipid ratio 1/50. At 37°C under stirring (800 rpm), polydispersity and vesicle size (in intensity) were measured after 20 min and one night.**

3.5. Fluorescence Microscopy

In order to characterize the peptide activity on the biological membrane, sequences labeled by fluorescent NBD were incubated with subconfluent epithelial cells (CHO) at 37°C and the peptide behavior was observed by fluorescence microscopy after 30 min or 1h. Considering the low solubility and membranotropic activity of **HCV6**, these experiments were only performed with **Tat-NT** as the reference and **HCV7-N**.

As already demonstrated by several groups, **Tat-NT** is able to cross the plasma membrane since NBD fluorescence (yellow) could be observed in the intracellular media after 30 min incubation (Figure 1). The punctiform staining observed in the cytoplasm shows vesicles formation, demonstrating that internalization by endocytosis could be involved as it has already been described[44,45].

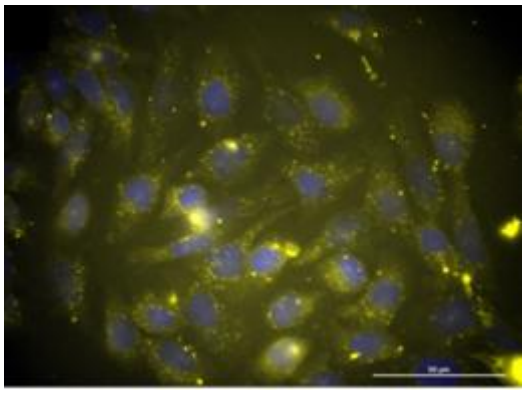

Figure 11: Pictures acquired by fluorescence microscopy for Tat-NT after 30 min incubation with CHO cells. Cells were incubated with 400 µL of a 100 µM for Tat-NT peptide TFA-free solution in PBS buffer for 30 min or 1 h at 37°C. Cells were fixed with 3% paraformaldehyde for 10 minutes and washed with PBS. After washing, cell nuclei were stained with DAPI (4,6-diamidino-2-phenylindole dihydrochloride) at 0.3µg/ml. Coverslips were mounted in Prolong® Gold Antifade Reagent

The experiments with **HCV7-N** led to the same conclusions. Indeed, NBD fluorescence and punctiform staining are observed in the cytoplasm after 30 min incubation (Figure 12). This

observation demonstrates the propensity of **HCV7-N** to cross a plasma membrane, probably involving endocytosis.

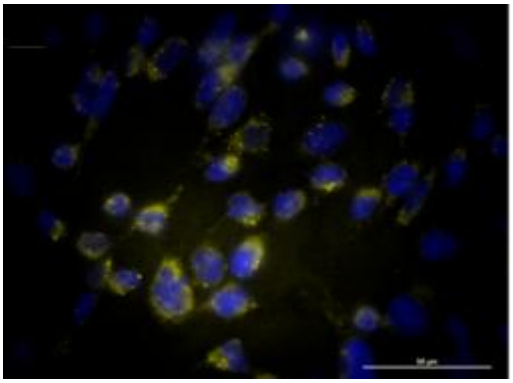

Figure 12: Pictures acquired by fluorescence microscopy for HCV7 after 30 min incubation with CHO cells. Cells were incubated with 400 µL of a 25 µM for HCV7-N **peptide TFA-free solution in PBS buffer for 30 min or 1 h at 37°C. Cells were fixed with 3% paraformaldehyde for 10 minutes and washed with PBS. After washing, cell nuclei were stained with DAPI (4,6-diamidino-2-phenylindole dihydrochloride) at 0.3µg/ml. Coverslips were mounted in Prolong® Gold Antifade Reagent..**

4. Discussion

4.1. HCV peptides structure in micelles

Conformational analysis performed on **HCV6** and **HCV7** by CD (Figure 1 and Table 3) pointed to a prevalence of unstructured states in water solution for both peptides. In the presence of DPC micelles as a mimetic of zwitterionic (mammalian) membranes, **HCV6** structure becomes more ordered (Figure 1a). Depending on the estimation method used, an increase of the α-helix or β-strand content is provided. The last suggestion, *i.e.* a high propensity of **HCV6** to adopt a β-sheet conformation could explain the observed low solubility of **HCV6** which, in that case, would be due to the formation of amyloid-like β-sheet aggregates. Unfortunately, this possibility could not be confirmed by NMR investigations because the peptide solubility is too low.

HCV7 showed a lower degree of structuration upon DPC micelle interaction. An increase of the β-strand content is provided by only one of the methods used for the estimation (Table 3). **HCV7** was also investigated in SDS micelles as mimetic of negatively charged membranes since DSC results clearly indicate that electrostatic interactions are crucial for **HCV7** membranotropic activity. CD spectrum acquired in SDS is very similar to that obtained in DPC (Figure 1b). From this result, it can be stated that the different membranotropic behavior of **HCV7** toward zwitterionic or anionic membranes is not driven by a conformational modification.

HCV7 conformation in the presence of DPC micelle was also investigated by solution NMR. We used a DPC micelle solution as mimetic of zwitterionic membranes since these, *i.e.* mammalian membranes, are the putative target of the peptide. Since CD analysis demonstrated minimal conformational differences of the peptide interacting with negatively charged SDS micelles compared to DPC, NMR analysis was limited to the last solution. The NMR analysis demonstrated the presence of β-turn structures along the central and C-terminal regions of the peptide in equilibrium with unordered conformations. There is no evidence of the β-strand structures estimated by the CD spectra. This is probably to attribute to the largely overlapping dichroic bands arising from β-turn and β-sheet structures.

4.2. HCV peptides membranotropic behavior

HCV6 membrane behavior was difficult to assess since its low solubility in water did not allow performing relevant DSC analyses. The solubility also seems to be a limiting factor for studying the **HCV6** membranotropic activity by spectrofluorescence since no insertion and/or internalization could be observed (Table 6) either with DMPC/DMPG 9/1 and DMPG LUVs. This lack of activity could be related to a low local concentration in contact with the membrane.

On the contrary, **HCV7** clearly interacts with lipids in the membrane as it has been demonstrated by DSC and structural analyses. This interaction seems to be more important with anionic lipids such as PG, creating fluid peptide-rich domains within the membrane. The absence of membrane modification with zwitterionic lipids such as PC suggests an electrostatic interaction, probably between the arginine residue and the phosphate group.

Spectrofluorescence assays show that **HCV7** is a membranotropic sequence, able to insert into the lipid bilayer and/or to cross it. Again, this behavior seems to be influenced by the presence of anionic residues in membrane since its activity could not be observed with pure DMPC vesicles. Unfortunately, the lack of reproducibility does not allow clearly defining the peptide membranotropic behavior. This low activity could be related to experimental conditions (DT concentration, peptide concentration) and/or to peptide properties (weak membrane interaction, secondary structure, partition equilibrium).

However, the fluorescence microscopy did demonstrate the **HCV7**'s propensity to cross the plasma membrane thus indicating its potential as a cell-penetrating agent. The peptide intake seems to involve endocytosis which could also explain the difficulties faced during internalization experiments with LUVs. Interestingly, the peptide seems to induce cytotoxic activity or cell's adhesion inhibition. A possible effect of NBD could not be excluded, thus it should be interesting to study the peptide internalization within cells using a different fluorescent probe[46] or immunofluorescence.

4.3. HCV peptides fusogenic activity

FRET assays and DLS analyses both state that **HCV6** is a fusogenic sequence whereas **HCV7** is not. The fusion or aggregation induced by **HCV6** seems weak and occurs at low rates. This low activity could be explained by an insufficient structuration in contact with membranes. Indeed, Wadhwani *et al.*[41] have shown that peptide fusogenic activity is directly correlated to its propensity to adopt a particular structure during the fusion process (being α-helix or β-structures). Thus, the lack of fusogenic activity for **HCV7** could be imputed to its prevailing random coil conformation in contact with lipids as it has been demonstrated by structural analyses.

In the case of **HCV6**, the low membranotropic activity could be explained by the too short sequence or the absence of important residues for the fusion process, remaining to be determined. Moreover the peptide membranotropic properties should certainly be correlated to combined effects of sequences rather than to the presence of a specific amino acid. This phenomenon could be associated to a cooperative type behavior, where the fusion peptide structuration occurs in contact with the membrane as the same time as the interactions of others sequences with the membrane or/and receptors. This hypothesis has been ascertained by Banerjee *et al*,[47] studying the synergetic relation between the MPER domain (C-terminal membrane proximal external region) and the folding of gp41 ectodomain monomers into an hairpin conformation followed by assembly into a hexamer. Concerning the HCV, a cooperative cascade of foldings and interactions involving several peptide sequences domains has been also postulated.[48] However, from a molecular point of view, the role of important residues

remains less explained even if the presence of hydrophobic (leucine) or aromatic (histidines) aminoacids and glycosylation are involved in the membranotropic properties.

5. Conclusion

Altogether, the techniques involved in this study allowed us to identify a new HCV membranotropic sequence (**HCV7**). This peptide seems to interact preferentially with anionic membrane components due to its arginine residue as it has been demonstrated for several CPPs. Even if its membrane behavior on LUVs has not been clearly assessed, experiments performed with cells did show its propensity to cross plasma membrane by endocytosis, thus confirming its potential as a cell-penetrating agent.

This study also confirms the **HCV6** fusogenic activity described in the literature thus supporting the hypothesis that this sequence corresponds to the HCV fusion peptide.

However, the two peptides' activity is lower than expected. This observation could be explained by the short sequences used, their lack of secondary structure and the absence of possibly important residues. Thus, it should be interesting to extend our study to longer HCV sequences folding into stable β-turns, which is generally the fusion peptide structure adopted within the protein, by keeping the cysteine residues for disulfide bond formation, or by lactamisation in order to constrain the sequences.

References

[1] C. Bechara, S. Sagan, Cell-Penetrating Peptides: 20 Years Later, Where Do We Stand?, FEBS Lett. 587 (2013) 1693–1702.

[2] Z. Guo, H. Peng, J. Kang, D. Sun, Cell-penetrating peptides: Possible transduction mechanisms and therapeutic applications (Review), Biomed. Reports. 4 (2016) 528–534.

[3] J. Durzynska, L. Przysiecka, R. Nawrot, J. Barylski, G. Nowicki, A. Warowicka, O. Musidlak, A. Gozdzicka-Jozefiak, Viral and Other Cell-Penetrating Peptides as Vectors of Therapeutic Agents in Medicine, J. Pharmacol. Exp. Ther. 354 (2015) 32–42.

[4] A. Falanga, M. Galdiero, S. Galdiero, Membranotropic cell penetrating peptides: The outstanding journey, Int. J. Mol. Sci. 16 (2015) 25323–25337.

[5] F. Simeoni, M.C. Morris, F. Heitz, G. Divita, Insight into the mechanism of the peptide-based gene delivery system MPG: Implications for delivery of siRNA into mammalian cells, Nucleic Acids Res. 31 (2003) 2717–2724.

[6] D. Moradpour, F. Penin, Hepatitis C Virus Proteins: From Structure to Function, in: Hepatitis C Virus: From Molecular Virology to Antiviral Therapy. Current Topics in Microbiology and Immunology, Vol 369, Springer, Berlin, Heidelberg, 2013: pp. 113–142.

[7] H. Freedman, M.R. Logan, J.L.M. Law, M. Houghton, Structure and Function of the Hepatitis C Virus Envelope Glycoproteins E1 and E2: Antiviral and Vaccine Targets, ACS Infect. Dis. 2 (2016) 749–762.

[8] R.F. Garry, S. Dash, Proteomics computational analyses suggest that hepatitis C virus E1 and pestivirus E2 envelope glycoproteins are truncated class II fusion proteins, Virology. 307 (2003) 255–265.

[9] M. Rodríguez-Rodríguez, D. Tello, J. Gómez-Gutiérrez, D.L. Peterson, F. Gavilanes, B.

Yélamos, Fusogenic properties of the Ectodomain of HCV E2 envelope protein, Biochim. Biophys. Acta - Biomembr. 1860 (2018) 728–736.

[10] G. Vieyres, X. Thomas, V. Descamps, G. Duverlie, A.H. Patel, J. Dubuisson, Characterization of the Envelope Glycoproteins Associated with Infectious Hepatitis C Virus, J. Virol. 84 (2010) 10159–10168.

[11] H.E. Drummer, I. Boo, P. Poumbourios, Mutagenesis of a conserved fusion peptide-like motif and membrane-proximal heptad-repeat region of hepatitis C virus glycoprotein E1, J. Gen. Virol. 88 (2007) 1144–1148.

[12] A.J. Pérez-Berná, M.R. Moreno, J. Guillén, A. Bernabeu, J. Villalaín, The membrane-active regions of the hepatitis C virus E1 and E2 envelope glycoproteins, Biochemistry. 45 (2006) 3755–3768.

[13] A.J. Pérez-Berná, G. Pabst, P. Laggner, J. Villalaín, Biophysical characterization of the fusogenic region of HCV envelope glycoprotein E1, Biochim. Biophys. Acta - Biomembr. 1788 (2009) 2183–2193.

[14] B. Pacheco, J. Gómez-Gutiérrez, B. Yélamos, C. Delgado, F. Roncal, J.P. Albar, D. Peterson, F. Gavilanes, Membrane-perturbing properties of three peptides corresponding to the ectodomain of hepatitis C virus E2 envelope protein, Biochim. Biophys. Acta - Biomembr. 1758 (2006) 755–763.

[15] D. Lavillette, E.-I. Pécheur, P. Donot, J. Fresquet, J. Molle, R. Corbau, M. Dreux, F. Penin, F.-L. Cosset, Characterization of Fusion Determinants Points to the Involvement of Three Discrete Regions of Both E1 and E2 Glycoproteins in the Membrane Fusion Process of Hepatitis C Virus, J. Virol. 81 (2007) 8752–8765.

[16] H.-F. Li, C.-H. Huang, L.-S. Ai, C.-K. Chuang, S.S.L. Chen, Mutagenesis of the fusion peptide-like domain of hepatitis C virus E1 glycoprotein: Involvement in cell fusion and virus entry, J. Biomed. Sci. 16 (2009) 89.

[17] S.R. Schwarze, A. Ho, A. Vocero-Akbani, S.F. Dowdy, In Vivo Protein Transduction: Delivery of a Biologically Active Protein into the Mouse, Science. 285 (1999) 1569–1572.

[18] A. Walrant, S. Cardon, F. Burlina, S. Sagan, Membrane Crossing and Membranotropic Activity of Cell-Penetrating Peptides: Dangerous Liaisons?, Acc. Chem. Res. 50 (2017) 2968–2975.

[19] S.W. Provencher, J. Gloeckner, Estimation of globular protein secondary structure from circular dichroism, Biochemistry. 20 (1981) 33–37.

[20] A. Micsonai, F. Wien, L. Kernya, Y.-H. Lee, Y. Goto, M. Réfrégiers, J. Kardos, Accurate secondary structure prediction and fold recognition for circular dichroism spectroscopy, Proc. Natl. Acad. Sci. 112 (2015) E3095–E3103.

[21] A. Micsonai, F. Wien, É. Bulyáki, J. Kun, É. Moussong, Y.H. Lee, Y. Goto, M. Réfrégiers, J. Kardos, BeStSel: A web server for accurate protein secondary structure prediction and fold recognition from the circular dichroism spectra, Nucleic Acids Res. 46 (2018) W315–W322.

[22] T.L. Hwang, A.J. Shaka, Water Suppression That Works. Excitation Sculpting Using Arbitrary Wave-Forms and Pulsed-Field Gradients, J. Magn. Reson. Ser. A. 112 (1995) 275–279.

[23] U. Piantini, O.W. Sorensen, R.R. Ernst, Multiple quantum filters for elucidating NMR coupling networks, J. Am. Chem. Soc. 104 (1982) 6800–6801.

[24] D. Marion, K. Wüthrich, Application of phase sensitive two-dimensional correlated spectroscopy (COSY) for measurements of 1H-1H spin-spin coupling constants in proteins,

Biochem. Biophys. Res. Commun. 113 (1983) 967–974.

[25] L. Braunschweiler, R.. Ernst, Coherence transfer by isotropic mixing: Application to proton correlation spectroscopy, J. Magn. Reson. 53 (1983) 521–528.

[26] J. Jeener, B.H. Meier, P. Bachmann, R.R. Ernst, Investigation of exchange processes by two dimensional NMR spectroscopy, J. Chem. Phys. 71 (1979) 4546–4553.

[27] D.J. States, R.A. Haberkorn, D.J. Ruben, A two-dimensional nuclear overhauser experiment with pure absorption phase in four quadrants, J. Magn. Reson. 48 (1982) 286–292.

[28] C. Bartels, T. Xia, M. Billeter, P. Güntert, K. Wüthrich, The program XEASY for computer-supported NMR spectral analysis of biological macromolecules, J. Biomol. NMR. 6 (1995) 1–10.

[29] K. Wüthrich, NMR of Proteins and Nucleic Acids, John Wiley & Sons: New York, 1986.

[30] G.R. Bartlett, Phosphorus Assay in Column Chromatography, J. Biol. Chem. 234 (1959) 466–468.

[31] A.A. Langham, H. Khandelia, Y.N. Kaznessis, How can a β-sheet peptide be both a potent antimicrobial and harmfully toxic? Molecular dynamics simulations of protegrin-1 in micelles, Biopolym. (Peptide Sci. 84 (2005) 219–231.

[32] M.R. Saviello, S. Malfi, P. Campiglia, A. Cavalli, P. Grieco, E. Novellino, A. Carotenuto, New insight into the mechanism of action of the temporin antimicrobial peptides, Biochemistry. 49 (2010) 1477–1485.

[33] P. Grieco, V. Luca, L. Auriemma, A. Carotenuto, M.R. Saviello, P. Campiglia, D. Barra, E. Novellino, M.L. Mangoni, Alanine scanning analysis and structure–function relationships of the frog-skin antimicrobial peptide temporin-1Ta, J. Pept. Sci. 17 (2011) 358–365.

[34] D.S. Wishart, B.D. Sykes, F.M. Richards, The chemical shift index: a fast and simple method for the assignment of protein secondary structure through NMR spectroscopy, Biochemistry. 31 (1992) 1647–1651.

[35] G. Van Meer, D.R. Voelker, G.W. Feigenson, Membrane lipids: Where they are and how they behave, Nat. Rev. Mol. Cell Biol. 9 (2008) 112–124.

[36] J.B. Rothbard, T.C. Jessop, R.S. Lewis, B.A. Murray, P.A. Wender, Role of Membrane Potential and Hydrogen Bonding in the Mechanism of Translocation of Guanidinium-Rich Peptides into Cells, J. Am. Chem. Soc. 126 (2004) 9506–9507.

[37] J.-M. Swiecicki, M. Di Pisa, F. Burlina, P. Lécorché, C. Mansuy, G. Chassaing, S. Lavielle, Accumulation of cell-penetrating peptides in large unilamellar vesicles: A straightforward screening assay for investigating the internalization mechanism, Biopolym. (Peptide Sci. 104 (2015) 533–543.

[38] T. Murayama, T. Masuda, S. Afonin, K. Kawano, T. Takatani-Nakase, H. Ida, Y. Takahashi, T. Fukuma, A.S. Ulrich, S. Futaki, Loosening of Lipid Packing Promotes Oligoarginine Entry into Cells, Angew. Chemie Int. Ed. 56 (2017) 7644–7647.

[39] S.-T. Yang, V. Kiessling, J.A. Simmons, J.M. White, L.K. Tamm, HIV gp41–mediated membrane fusion occurs at edges of cholesterol-rich lipid domains, Nat. Chem. Biol. 11 (2015) 424–431.

[40] D.K. Struck, D. Hoekstra, R.E. Pagano, Use of resonance energy transfer to monitor membrane fusion, Biochemistry. 20 (1981) 4093–4099.

[41] P. Wadhwani, J. Reichert, J. Bürck, A.S. Ulrich, Antimicrobial and cell-penetrating peptides induce lipid vesicle fusion by folding and aggregation, Eur. Biophys. J. 41 (2012) 177–187.

[42] J. Yang, C.M. Gabrys, D.P. Weliky, Solid-State Nuclear Magnetic Resonance Evidence for an Extended β Strand Conformation of the Membrane-Bound HIV-1 Fusion Peptide, Biochemistry. 40 (2001) 8126–8137.

[43] M. Soleymani-Goloujeh, A. Nokhodchi, M. Niazi, S. Najafi-Hajivar, J. Shahbazi-Mojarrad, N. Zarghami, P. Zakeri-Milani, A. Mohammadi, M. Karimi, H. Valizadeh, Effects of N-terminal and C-terminal modification on cytotoxicity and cellular uptake of amphiphilic cell penetrating peptides, Artif. Cells, Nanomedicine, Biotechnol. (2017). doi:10.1080/21691401.2017.1414823.

[44] I.M. Kaplan, J.S. Wadia, S.F. Dowdy, Cationic TAT peptide transduction domain enters cells by macropinocytosis, J. Control. Release. 102 (2005) 247–253.

[45] J.P. Richard, K. Melikov, H. Brooks, P. Prevot, B. Lebleu, L. V. Chernomordik, Cellular uptake of unconjugated TAT peptide involves clathrin-dependent endocytosis and heparan sulfate receptors, J. Biol. Chem. 280 (2005) 15300–15306.

[46] S.-T. Yang, E. Zaitseva, L. V. Chernomordik, K. Melikov, Cell-penetrating peptide induces leaky fusion of liposomes containing late endosome-specific anionic lipid, Biophys. J. 99 (2010) 2525–2533.

[47] K. Banerjee, D.P. Weliky, Folded Monomers and Hexamers of the Ectodomain of the HIV gp41 Membrane Fusion Protein: Potential Roles in Fusion and Synergy Between the Fusion Peptide, Hairpin, and Membrane-Proximal External Region, Biochemistry. 53 (2014) 7184–7198.

[48] A. Sabahi, S.L. Uprichard, W.C. Wimley, S. Dash, R.F. Garry, Unexpected Structural Features of the Hepatitis C Virus Envelope Protein 2 Ectodomain, J. Virol. 88 (2014) 10280–10288.